

Fibrillin-2, tenascin-C, matrilin-2, and matrilin-4 are strongly expressed in the epithelium of human granular and lattice type I corneal dystrophies

Eszter Szalai,¹ Szabolcs Felszeghy,² Zoltán Hegyi,² László Módis Jr,¹ András Berta,¹ Kai Kaarniranta^{3,4}

(The first two authors contributed equally to the work)

¹Department of Ophthalmology, University of Debrecen, Medical and Health Science Center, Debrecen, Hungary; ²Department of Anatomy, Histology and Embryology, University of Debrecen, Medical and Health Science Center, Debrecen, Hungary;

³Department of Ophthalmology, Institute of Clinical Medicine, University of Eastern Finland, Kuopio, Finland; ⁴Department of Ophthalmology, Kuopio University Hospital, Kuopio, Finland

Purpose: To determine the extracellular matrix proteins involved in the formation of human granular and lattice type I corneal stromal dystrophies, the expression patterns of fibrillin-2, tenascin-C, matrilin-2, and matrilin-4 were compared in human corneal stromal dystrophy samples.

Methods: Ten cases of granular dystrophy, 7 cases of lattice dystrophy, and 6 normal corneal buttons collected during corneal transplantation were examined for their expression patterns of fibrillin-2, tenascin-C, matrilin-2, and matrilin-4 by immunohistochemistry.

Results: Highly elevated fibrillin-2, tenascin-C, matrilin-2, and matrilin-4 were observed in the epithelial layer of both granular and lattice type I dystrophies. Fibrillin-2, tenascin-C, and matrilin-4 in the granular dystrophy and all antibodies in the lattice dystrophy showed statistically significant staining in the corneal stroma ($p < 0.05$). Interestingly, fibrillin-2, matrilin-2, and matrilin-4 stained significantly in amyloid plaques of lattice type I dystrophy.

Conclusions: Fibrillin-2, tenascin-C, matrilin-2, and matrilin-4 may be markers of the pathogenesis of either granular or lattice type I corneal dystrophy, as revealed by immunohistochemical analysis. Each molecule seems to be involved in the regeneration and reorganization of the corneal matrix in granular and lattice type I dystrophies.

Stromal corneal dystrophies are primary, genetically determined, bilateral, noninflammatory disorders affecting the stromal layer of the cornea. Granular type I corneal dystrophy (corneal dystrophy Groenouw type I, OMIM 121900) is an autosomal-dominant disease characterized by multiple stromal opacities [1]. Its onset usually occurs during childhood, and the rate of clinical disease progression varies between individuals. Lattice type I cornea dystrophy (Biber-Haab-Dimmer dystrophy, OMIM 122200) has autosomal-dominant inheritance and typically presents in the first decade of life [1]. Both granular and lattice type I stromal dystrophies have been linked to allelic mutations in the transforming growth factor- β (TGF- β) induced gene-h3 (*BIGH3*) on chromosome 5q31 [2-4]. The abnormal gene product (protein) accumulates in the corneal layers and forms deposits that are generally characteristic of the corneal dystrophy type [5].

The corneal stroma is composed of keratocytes (2%–3% of the total stromal volume) [6], extracellular matrix (ECM) molecules and stromal nerves. Corneal transparency and

function are based on the special composition and assembly of the extracellular matrix structures as well as on the cell-cell and cell-ECM interactions [7]. Fibrillins play an important role in maintaining tissue integrity and homeostasis through the modulation of TGF- β and bone morphogenetic protein signaling [8]. Fibrillin-2 binds to other ECM proteins, forming microfibrils, and is mostly expressed during embryogenesis [9]. Tenascin-C is a hexameric ECM glycoprotein, and its expression is restricted to the fetal period of development [10]. It is responsible for various dynamic cellular activities, including cell adhesion [11], de-adhesion [12,13], inflammation [10], tissue remodeling [10], angiogenesis [14], migration [10], proliferation [15], and growth [11]. Enhanced expression of both fibrillin-2 and tenascin-C has been observed in adults with fibroproliferative conditions, such as wound healing and sclerosis [9,10,16]. Matrilin-2, discovered by Deák et al. [17], is the largest member of an extracellular matrix adaptor protein family of proteins that contain von Willebrand factor A-like domains [18]. Matrilins can connect to different types of collagenous and noncollagenous ECM structures, participate in various protein-protein interactions and, thus, determine the tissue integrity [19]. Matrilin-4 is the most recently identified member of the matrilin superfamily [20]. The trimer

Correspondence to: Professor Kai Kaarniranta, Department of Ophthalmology, Kuopio University Hospital, P.O. Box 1777, FIN-70211, Kuopio, Finland; Phone: +358-17-172485; FAX: +358-17-172486; email: Kai.Kaarniranta@kuh.fi

matrilin-4 is a component of dense and loose connective tissues, bone, articular cartilage and nervous tissues and associates with basement membranes [21].

To the best of our knowledge, this is the first study to determine the expression pattern of fibrillin-2, tenascin-C, matrilin-2, and matrilin-4 in these corneal stromal dystrophies.

METHODS

Patients and tissue specimens: Tissue samples were obtained from 12 patients who underwent penetrating keratoplasty. Donor corneas obtained from the Cornea Bank Debrecen (Department of Ophthalmology, University of Debrecen, Medical and Health Science Centre) served as normal control corneas. The study included 23 total cases: 10 cases of granular type I dystrophy (7 patients), 7 cases of lattice type I dystrophy (5 patients), and 6 corneal buttons (6 patients) with a normal fibrillin-2, tenascin-C, matrilin-2, and matrilin-4 staining profile.

Antibodies: Monoclonal mouse antibodies against fibrillin-2 (clone 48; MAB2642, 1:250; Millipore, Bedford, MA) and tenascin-C (DB7; ab86182, 1:50; Abcam, Cambridge, UK), and polyclonal rabbit antibodies against matrilin-2 (ARP57667_P050, 1:300; Aviva Systems Biology, Corp., San Diego, CA) and matrilin-4 (ab106379, 1:300; Abcam) were used for immunohistochemistry.

Light microscopy: After corneal button removal, tissue samples were immediately fixed in formalin (10%, pH 7.2) and embedded in paraffin, and then 5–7 μm thick longitudinal sections were cut (Leitz 1208 microtome; Wild Leitz, GmbH, Wetzlar, Germany). Paraffin sections were mounted on Superfrost Plus slides (Menzel-Gläser, Germany) and left to dry overnight. Sections were deparaffinized with xylene and rehydrated through a graded series of ethanol and distilled water. For light microscopy analysis after rehydration, the sections were stained with hematoxylin and eosin (H&E) according to the manufacturer's protocol and covered with DPX (BDH Laboratory Supplies, Poole, England). Congo Red staining was applied to show the presence of amyloid.

Analysis of staining: The histological morphology of the corneal samples was evaluated by two independent researchers (E.S., S.F.) at 20 \times magnification in routine hematoxylin-eosin-stained and in Congo Red sections from each individual cases.

Immunohistochemical staining: For immunohistochemical analysis after rehydration, slides were treated with 3% hydrogen peroxide to block the endogenous peroxidase activity. For immunostaining, Histostain-Plus kits for mouse and broad-spectrum primary antibodies (Invitrogen, Camarillo, CA) were used. The sections were incubated in serum-blocking solution for 30 min at room temperature. Fibrillin-2, tenascin-C, matrilin-2, and matrilin-4 primary antibodies were applied overnight at dilutions of 1:250, 1:50,

1:300, and 1:300, respectively, in TBS (pH 7.4) at 4 °C. Then, the slices were washed twice with TBS, and the biotinylated secondary antibody (1:200 dilution) was applied for 30 min at room temperature. After washing with TBS, the samples were treated with enzyme conjugate for 30 min at room temperature. Reactions were visualized by the diaminobenzidine (DAB) immunoperoxidase technique using a DAB detection kit (Invitrogen). All kit solutions were diluted in TBS, and the incubations for the DAB chromogen procedure were performed in humid chambers at room temperature according to the manufacturer's protocol. Nuclei were counterstained with Harris' hematoxylin (Merck, Darmstadt, Germany). The sections were dehydrated in a graded series of ethanol and xylene and mounted with DPX (BDH Laboratory Supplies). The slides were observed with a light microscope (BX40; Olympus, Tokyo, Japan) equipped with a digital camera (DP50; Olympus), and digitized images were processed using Adobe Photoshop CS4 (Adobe Systems Inc., CA).

We performed preabsorption reaction of matrilin-2 antibody using specific blocking peptide (Aviva Systems Biology, San Diego). The lack of immunostaining in these sections confirms the specificity of our antibody. This type of negative control would be ideal and necessary in the characterization and evaluation of antibodies used but it was not possible to obtain the purified antigen from companies, therefore control sections were stained in same way but the primary antibody was omitted and replaced by non-immune IgG (Sigma Aldrich, St. Louis, MO). No immunostaining was observed in these sections indicating that our immunostaining protocol is specific.

Immunofluorescence: To examine the colocalization of matrilin-2 and fibrillin-2 in corneal epithelial cell double immunostaining protocol has been performed. Tissue sections were fixed as described above. To prevent the nonspecific staining, before the antibody treatments the slides were incubated in serum-blocking solution for 1 h at room temperature. Subsequently, the slides were incubated with a mixture of antibodies, that contained anti-matrilin-2 (diluted 1:250) and anti fibrillin-2 (diluted 1:300) antibodies. After 2 days long incubation at 4 °C with the primary antibody solution the slides were rinsed in PBS and, the mixture of secondary antibodies (Alexa Fluor 488 anti-mouse Ig and the Alexa Fluor 546 anti-rabbit Ig; Invitrogen, Camarillo, CA) has been placed to samples for 2 h at room temperature. The slides were washed and the nuclei were stained using DAPI (4,6-diamidino-2-fenilindole, dihydrochloride; 1:1,000; Molecular Probes Camarillo, CA) in PBS containing 0.1% saponin for 30 min and covered with Vectashield mounting Media (Vector Laboratories, Burlingame, CA). As negative controls for each double label, the same procedure as above was followed except that one of the primary antibodies was omitted. No immunostaining was seen in these sections [22].

Confocal microscopy: Acquired and presented images were representative of all the samples examined with a Olympus FV1000 confocal microscope (Olympus, Tokyo, Japan). Using 60× oil immersion lens single 1 μm thick section were scanned. The confocal settings were identical for all scans and kept constant during imaging. The recorded images were processed by Adobe Photoshop CS4 software.

Computer-assisted image analysis: The immunostained results were recorded as digital images using the setup described above. From each immunohistochemical slide, representative fields (100× objective) were captured. The settings of the microscope and camera were kept constant during capturing of the pictures, and digitalized images were analyzed in **Image J** software with macroinstructions for analyzing each captured area. The total intensity of DAB developed immunohistochemical staining of different antibodies used (Fibrillin-2/Tenascin-C/Matrilin-2 and -4), was measured for each region of interest (ROI). Pictures were recorded from 5 different randomly selected individual cases in each groups and on 5 sections from each of them independent gray intensity of ROIs (size approximately 5 μm²) was determined at two different locations of the corneal epithelium (basal and suprabasal cell layers) and in the subepithelial and deep zones of the corneal stroma.

Statistical analysis: Data were analyzed using the SPSS software version 11.0.05 (SPSS Inc., Chicago, IL). Significant differences in immunohistochemical staining intensity were determined by the Mann–Whitney U-test; differences with $p < 0.05$ were considered significant.

RESULTS

Histopathology: Figure 1 shows the clinical appearance of lattice type I (Figure 1A) and granular type I corneal dystrophy (Figure 1B,C). Figure 1D shows longitudinally sectioned granular type I stromal dystrophy after H&E staining. Typical of granular type I stromal dystrophy, multiple eosinophilic granules (asterisks) in the ground substance of the corneal stroma were observed. Figure 1E shows the amyloid plaques characteristic of lattice type I dystrophy. The deposits were variable in size, located in the mid- to deep stroma. Figure 1F shows the optical anisotropy of amyloids. Note the characteristic yellow-green birefringence after Congo Red staining under polarized light microscopy (arrowheads), indicating that these structures are amyloid in nature. The immunostainings of the anti-matrilin-2 and anti-fibrillin-2 antibodies were confirmed to localize in corneal epithelial layer analyzed by a single laser scanning confocal microscopy (Figure 1G-J).

Immunohistochemistry: The immunolocalization and staining intensity of fibrillin-2, tenascin-C, matrilin-2, and matrilin-4 in normal, granular type I and lattice type I stromal dystrophy corneas are summarized in Table 1.

Fibrillin-2—In normal corneal specimens, some corneal epithelial cells showed moderate cytoplasmic immunoreactivity (Figure 2A), although suprabasal and basal epithelial expression was significantly weaker in normal sections than in granular type I dystrophy ($p < 0.0001$ for both; Mann–Whitney U test) and in lattice type I corneal dystrophy ($p < 0.0001$ for both). The expression of fibrillin-2 in the basal cell layer and the superficial squamous cell layer of the corneal epithelium was intense in granular type I dystrophy (Figure 2B). No immunoreactivity was observed in Bowman’s membrane. Stromal deposits showed intense immunolocalization of fibrillin-2, but the ground substance of the stroma between the granules did not stain with the fibrillin-2 antibody ($p < 0.0001$ for both). Nearly as intense cytoplasmic immunoreactivity was found in the basal epithelial cells in lattice type I dystrophy as in those of granular type I dystrophy. Immunopositive cells formed a relatively continuous border between the epithelium and Bowman’s layer (Figure 2C). The anterior stroma and the amyloid plaques showed definitive immunoreactivity for fibrillin-2.

Tenascin-C—Normal corneal buttons showed mild immunolocalization for tenascin-C in the corneal epithelium (Figure 3A). In granular type I corneal dystrophy, epithelial cells stained intensely for tenascin-C ($p < 0.0001$ for both; Figure 3B). Bowman’s membrane did not display any immunopositivity for this protein. Stromal staining was stronger and statistically significant in the stromal deposits ($p < 0.0001$ for both) compared with between the granules. In basal epithelial cells, tenascin-C showed moderate immunolocalization in lattice type I dystrophy ($p < 0.0001$; Figure 3C). In Bowman’s layer, immunoreactivity was absent. Some mild immunostaining was detectable in the corneal stroma, but the immunoreactivity found in the amyloid deposits was absent or mild and, thus, nonspecific ($p = 0.912$, subepithelial).

Matrilin-2—Mild immunopositivity for matrilin-2 was found in normal samples (Figure 4A). In granular type I dystrophy, corneal epithelium showed intense, statistically significant intracellular reactions for matrilin-2, especially in wings and basal cells ($p < 0.0001$ for both). Figure 4B shows the focal thinning of Bowman’s layer in granular dystrophy. Stromal expression of matrilin-2 was observed, mainly in the corneal granules ($p = 0.248$, subepithelial; $p = 0.190$, deep). In lattice type I corneal dystrophy cases, diffuse but intense immunoreactivity for matrilin-2 was found in the enlarged basal epithelial cells ($p < 0.0001$; Figure 4C). The thinned or absent Bowman’s membrane showed no immunostaining. Corneal stroma in the amyloid deposits was mildly positive, and posterior stroma showed mild to moderate immunoreactivity in some lattice type I dystrophy cases, this difference was statistically significant ($p = 0.0001$).

Matrilin-4—In normal corneal specimens, mild immunoreactivity was detected for matrilin-4 in corneal

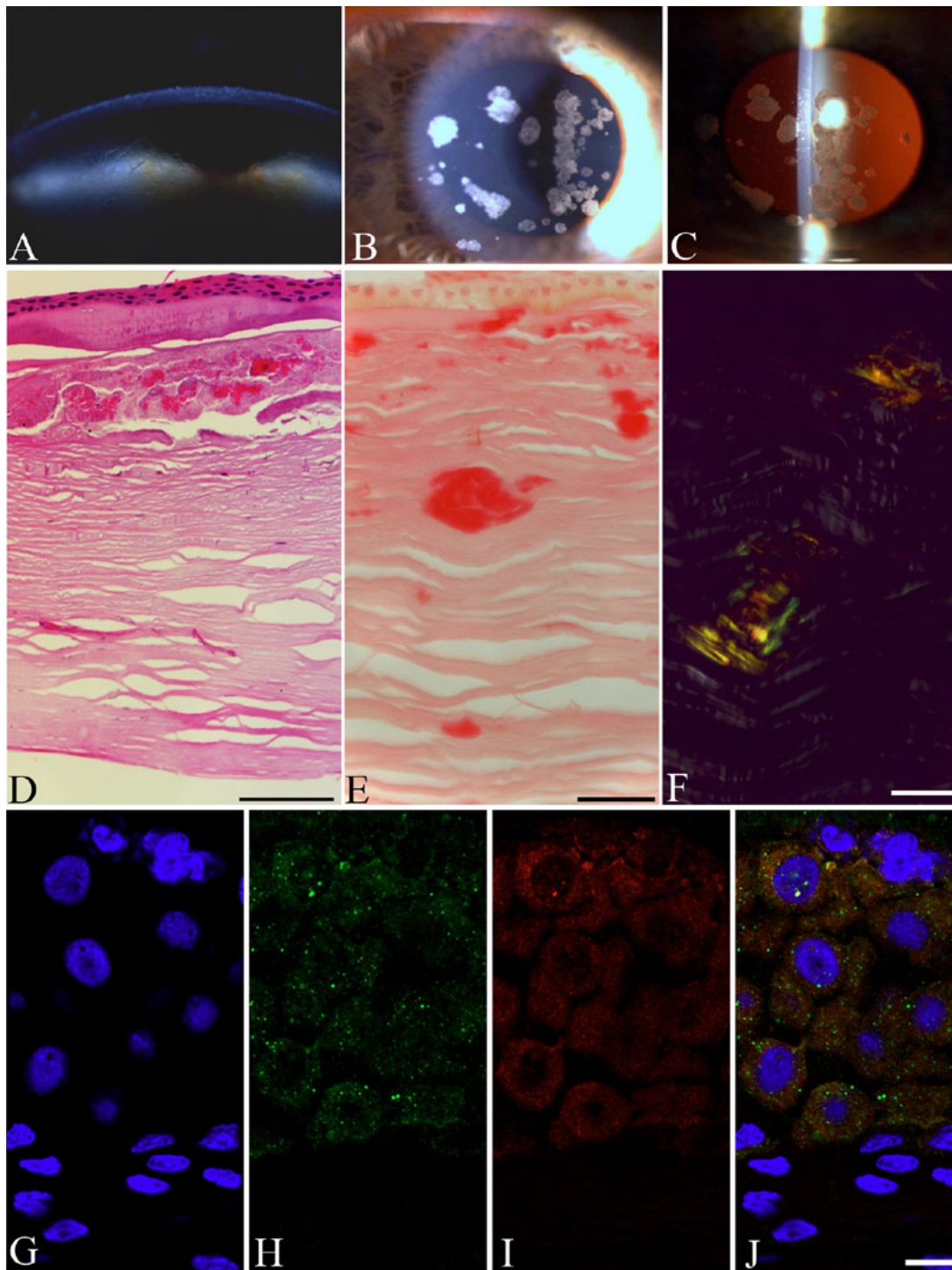


Figure 1. Granular and lattice type I dystrophies: biomicroscopic and histopathologic findings. The clinical appearance of lattice corneal dystrophy (A). The branching dots and lines, representing amyloid deposits, are typical in the corneal stroma. Granular corneal dystrophy under slit lamp and retroillumination (B). Well defined, white granules are present in the central corneal stroma (C). Histological section of the granular type I corneal button (H&E) (D). The deposits are observed in the sub-Bowman layer in the stroma. The section of lattice corneal dystrophy stains weak with Congo Red (E). Stromal fusiform amyloids stain with Congo red (F) and show birefringence under polarized light. The colocalization of matrilin-2 and fibrillin-2 in normal corneal epithelium is presented in G-J. High magnification microphotographs of single laser scanning confocal optical sections (1 μm) demonstrating the immunolocalization of the anti-matrilin-2 (H, green) and anti-fibrillin-2 (I, red) antibody in corneal epithelial layer. The nuclei are blue on each images presented (G-J). Note that no nuclear staining is present on the merged image (J) preclude the possibility of nonspecific reaction (internal control). Around the smaller DAPI labeled nucleus yellow color may indicate the colocalization of these two antibodies used. Scale bars for light and polarized microscopic images are 100 μm , for confocal images; 10 μm .

TABLE 1. IMMUNOLocalIZATION OF FIBRILLIN-2, MATRILIN-2, MATRILIN-4, AND TENASCIN-C IN NORMAL AND STROMAL DYSTROPHY CORNEAS (MAXIMUM AND MINIMUM GRAY LEVELS ARE 0 AND 255, RESPECTIVELY).

Antibody	Control						Granular type I dystrophy						Lattice type I dystrophy					
	Epithelium			Stroma			Epithelium			Stroma			Epithelium			Stroma		
	Suprabasal	Basal	Subepithelial	Deep	Suprabasal	Basal	Subepithelial	Deep	Suprabasal	Basal	Subepithelial	Deep	Suprabasal	Basal	Subepithelial	Deep		
Fibrillin-2 p*	205.97±3.95	188.42±3.06	168.09±5.83	167.66±9.54	116.37±6.34	54.55±2.5	110.30±5.21	<0.0001	<0.0001	104.08±4.04	44.78±2.22	<0.0001	158.6±5.37	0.001	158.10±6.85	0.012		
Tenascin-C p*	165.49±5.50	140.41±5.29	163.9±5.54	223.25±3.79	110.12±5.68	49.39±2.27	100.58±5.75	100.69±5.11	<0.0001	150.93±4.62	102.91±5.3	<0.0001	163.34±7.47	0.912	156.8±6.19	<0.0001		
Matrilin-2 P*	149.87±4.75	158.29±7.86	130.68±4.49	151.45±6.06	105.5±4.56	62.74±3.41	135.39±6.65	156.41±7.41	0.190	131.06±3.5	94.95±4.07	<0.0001	139.01±5.63	0.002	140.39±4.55	0.0001		
Matrilin-4 P*	162.21±6.55	165.07±7.13	223.09±2.41	222.54±2.84	102.54±4.82	85.13±3.82	119.48±4.76	115.56±4.59	<0.0001	125.90±4.2	91.26±4.46	<0.0001	134.44±5.93	<0.0001	132.28±4.13	<0.0001		

*Mann-Whitney U test (control versus granular/lattice dystrophy).

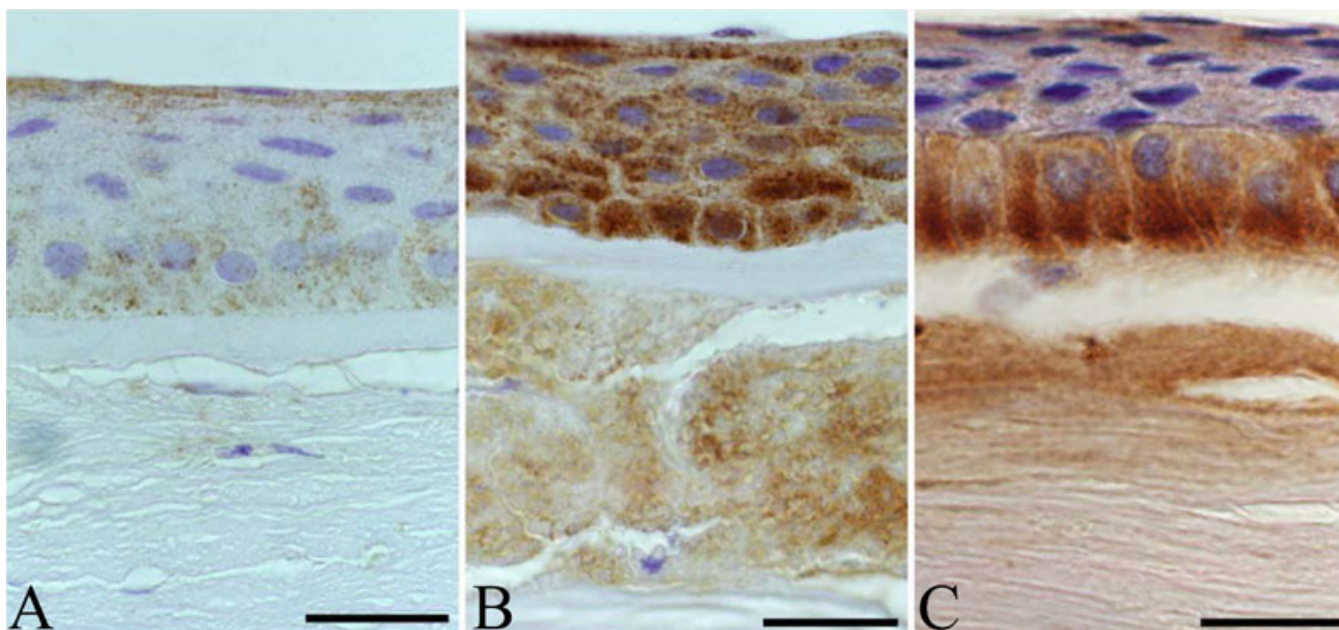


Figure 2. Comparison of expression patterns of fibrillin-2 in healthy, granular type I and lattice type I stromal dystrophy corneal buttons, and the colocalization of matrilin-2 and fibrillin-2 in corneal epithelium. Healthy samples showed mild immunolocalization in superficial and basal epithelial layers (A). In addition to the strong epithelial immunopositivity of fibrillin-2 in granular dystrophy, marked labeling was observed in stromal granules (B). In lattice corneal dystrophy, continuous cytoplasmic staining was found in the base of the basal columnar cells (C). Scale bar 100 μ m.

epithelium (Figure 5A). In the epithelial layer of granular type I dystrophy, diffuse, intense but discontinuous cytoplasmic immunoreactivity for matrilin-4 was found ($p < 0.0001$ for both). Note the absence of Bowman's membrane in Figure 5B. Deposits in the corneal stroma were positive for matrilin-4, and some stromal cells between the granules showed an irregular and mild expression pattern ($p < 0.0001$ for both). The superficial and basal epithelial cells displayed statistically significant, mild to moderate immunostaining for matrilin-4 in lattice type I dystrophy cases ($p < 0.0001$ for both; Figure 5C). Bowman's membrane, where present, was negative for matrilin-4. The anterior and posterior third of corneal stroma ($p = 0.945$ and 0.101 , respectively) and amyloid plaques showed intense and statistically significant immunolocalization of matrilin-4 in lattice type I dystrophy.

DISCUSSION

The present study investigated the expression patterns of fibrillin-2, tenascin-C, matrilin-2, and matrilin-4 in granular and lattice type I corneal stromal dystrophy samples. Unexpectedly, significantly higher immunoreactivity was detected for every antibody in the corneal epithelium in both types of dystrophy compared to the normal control samples. In the corneal stroma, stronger immunostaining for tenascin-C was found in the granular type I dystrophy group than in the control samples or lattice dystrophy group.

In granular type I corneal dystrophy, eosinophilic deposits primarily accumulate in the corneal stroma as a result of genetic mutation but also can be found in the epithelial layer

[23]. Accordingly, we observed moderate immunopositivity for fibrillin-2 in the basal and superficial epithelial cells. Fibrillins are produced by fibroblasts physiologically in developing or in regenerating tissues. In granular dystrophy, enhanced expression of fibrillin-2 can be explained by the increased ECM production and the multiple functions of fibrillins in ECM stabilization, in which they form microfibrils that associate with basement membranes and elastic fibers [24]. Additionally, modified BIGH3 proteins are thought to promote the adhesion, migration, and proliferation of epithelial cells and fibroblasts more efficiently than the wild type [25-27]. Mutant BIGH3 protein-related peptides contribute to amyloid formation by assembling β -sheet-rich oligomeric structures in lattice type I dystrophy corneas [28]. In accord with other studies, we also demonstrated the appearance of fibrillin-2 in amyloid plaques [29,30]. Basal cells of the corneal epithelium, which secrete the epithelial basement membrane, strongly expressed fibrillin-2 in lattice type I dystrophy, suggesting an ongoing healing process or fibrogenesis. In normal specimens, slight immunolocalization for fibrillin-2 was occasionally observed in some epithelial cells, which was significantly weaker than those in the dystrophy samples. In addition, two papers have reported immunopositivity for fibrillin-2 in the epithelial basement membrane of normal buttons [29,31].

Epithelial erosions have been described both in granular and in lattice type I dystrophy [32]. Increased expression of fibrillin-2 in the corneal epithelial cells may indicate epithelial

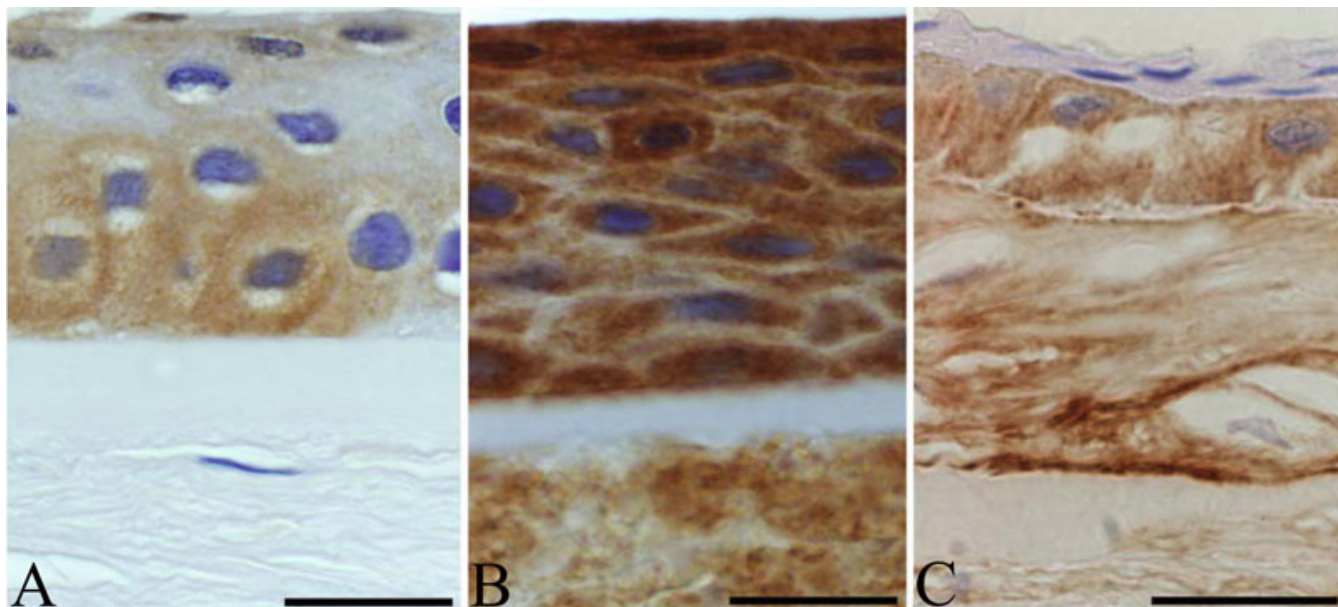


Figure 3. Comparison of the expression patterns of tenascin-C in healthy, granular type I, and lattice type I stromal dystrophy corneal buttons. Cytoplasmic immunolabeling in normal sections was only observed in some basal epithelial cells (A). In granular dystrophy, diffuse, marked immunostaining was recorded in the epithelial layers and in the stromal granules (B). Basal epithelium showed moderate immunostaining for tenascin-C in lattice dystrophy (C). Scale bar 100 μ m.

wound healing. Brinckman et al. [16] attributed the co-expression of fibrillin-2 and tenascin-C in wound healing to altered cell adhesion in ECM. In our study, similar expression patterns of fibrillin-2 and tenascin-C were found in granular type I dystrophy but not in lattice dystrophy. We detected stronger immunolocalization for tenascin-C in corneal epithelial cells and stromal granules in granular type I dystrophy specimens compared to the normal samples. This finding supports our assumption of decreased cell adhesion as a prominent feature of granular type I stromal dystrophy corneas. Tenascin-C immunopositivity in inflammation [33], active scarring [33,34], angiogenesis [35] and bullous keratopathy [36,37] have been documented. In developmental studies, tenascin-C is consistently detected in neonatal corneas, but it is limited to the limbus in adults [38,39]. In lattice type I dystrophy, moderate immunolocalization for tenascin-C was observed in all epithelial layers. One conspicuous finding of this study was the absent or weak immunopositivity of tenascin-C in the amyloid deposits. Similarly to other authors, we did not find this glycoprotein in normal central corneas [31,33,40], although some immunopositivity was observed in the epithelial cell layers. It should be noted that we used the monoclonal antibody DB7 against tenascin-C [41] and that the tenascin-C variants have different expression patterns [33,38].

Matrilins are recently identified adaptor proteins, but few studies have investigated their presence and function in the human cornea [31,39]. Matrilin-2, the non-collagenous basement membrane component, colocalizes with microfibrils and connects to fibrillin-2 [42]. In this study, mild

to moderate matrilin-2 expression was observed in the epithelial layer and in the stromal deposits in granular type I dystrophy, the expression patterns of fibrillin-2 and matrilin-2 were similar. This result also supports the notion that the regeneration and reorganization of the ECM that occur in granular type I dystrophy might be analogous to those of the wound healing process. Matrilin-2 functions in early cell differentiation during embryonal development, promotes axonal growth and Schwann cell migration during peripheral nerve regeneration [43], modulates wound healing in the skin [44] and plays a role in tumor development [45,46].

We observed diffuse, marked immunoreactivity for matrilin-2 in the epithelial cells of lattice type I dystrophy samples, but only slight reactivity in the stromal amyloid deposits. Posterior stroma also showed some mild immunostaining for matrilin-2 in lattice stromal dystrophy. Normal corneal epithelium and stroma exhibited mild immunopositivity for matrilin-2; however, two previous studies demonstrated immunolocalization of this oligomeric protein in the epithelial basement membrane in adult corneas [31,39]. Matrilin-4 staining in the stromal granules was less pronounced in granular type I dystrophy than the matrilin-2 reactivity. In contrast, amyloid deposits showed stronger immunolocalization for matrilin-4 than for matrilin-2 in lattice type I dystrophy, highlighting the difference in expression patterns between these two adaptor proteins in this disease. However, matrilin-2 and -4 arise from a common precursor, which suggests a close association between their tissue localization and functional roles [21]. Matrilin-4 is expressed in most tissue locations where any of the other

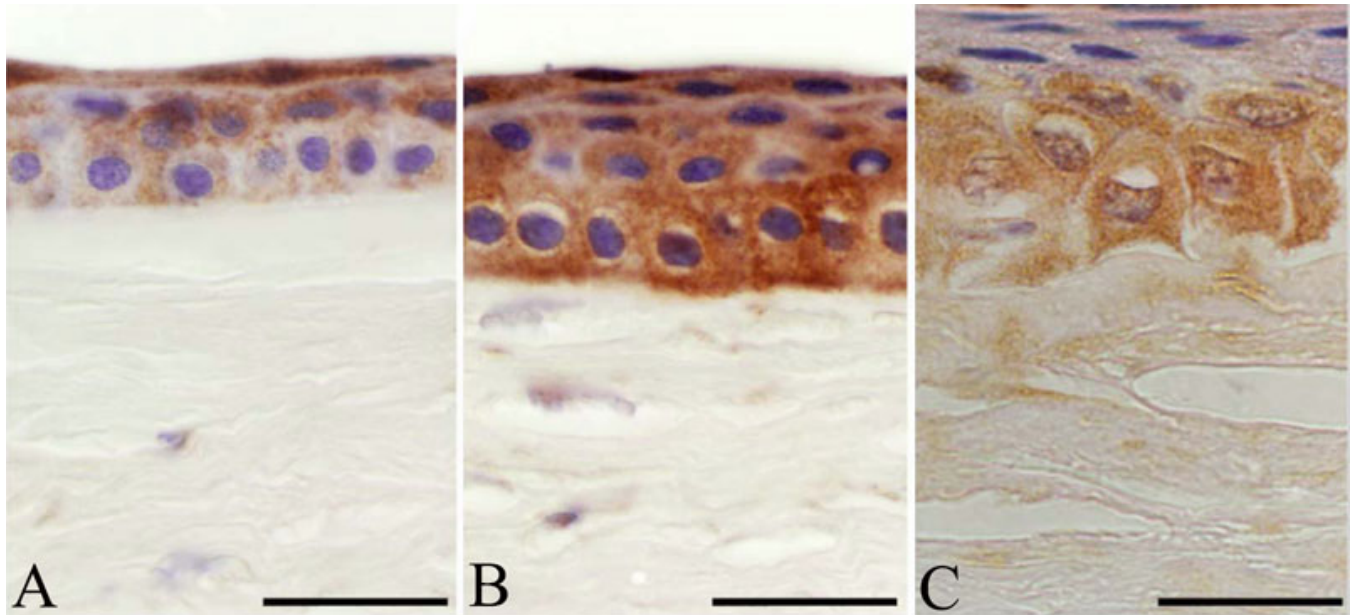


Figure 4. Comparison of the expression patterns of matrilin-2 in healthy, granular type I, and lattice type I stromal dystrophy corneal buttons. In normal controls, matrilin-2 was present in most corneal epithelial layers (A). Intense epithelial immunopositivity was observed in granular dystrophy. Focal thinning or loss of Bowman's layer was also apparent (B). Enlarged immunopositive basal cells in corneal epithelium with mild stromal staining were observed in lattice dystrophy (C). Scale bar 100 μ m.

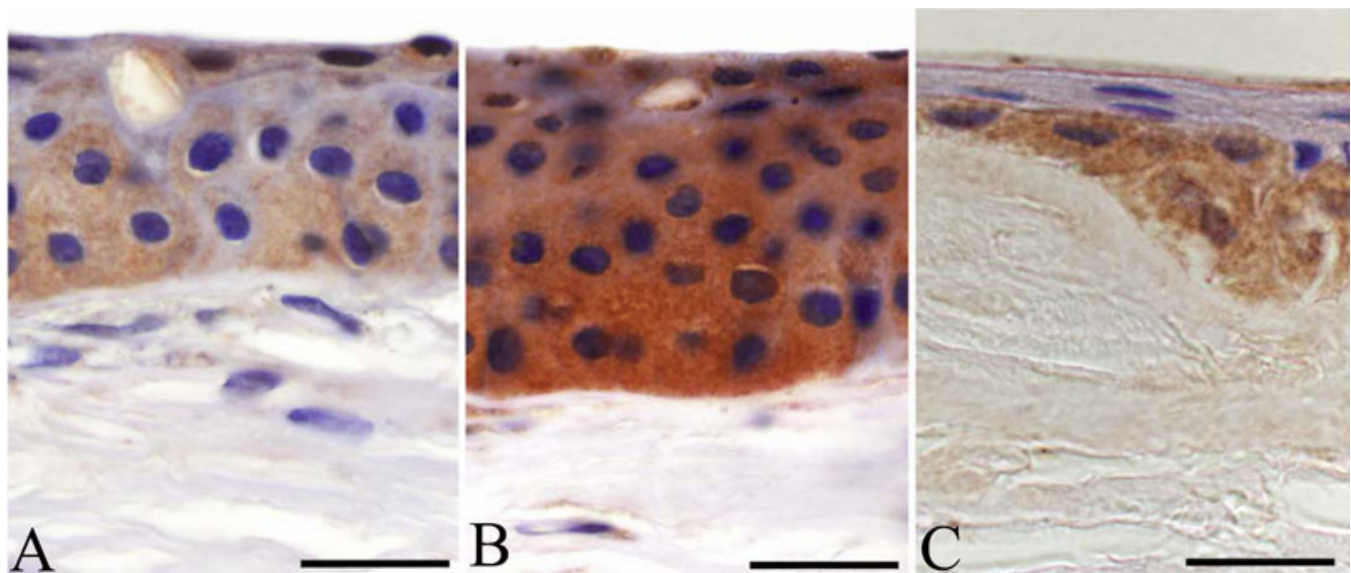


Figure 5. Comparison of the expression patterns of matrilin-4 in healthy, granular type I, and lattice type I stromal dystrophy corneal buttons. Some immunolabeling was recorded in healthy corneal epithelium (A). In granular dystrophy, all epithelial layers were positive for matrilin-4, and no Bowman's layer was present under the epithelial basement membrane (B). Altered epithelial cell morphology in the basal layer was observed, with strong basal immunolabeling for matrilin-4 in lattice type I dystrophy (C). Scale bar 100 μ m.

matrilins are present [21]. Further studies focusing on the difference between the roles of matrilin-2 and matrilin-4 are necessary to explain their different expression patterns in granular and lattice type I dystrophies. Matrilin-4 immunoreactivity has been observed in the epithelial basement membrane in adult corneas [31,39], although we

only found weak immunostaining in the epithelial cells in control specimens.

In conclusion, fibrillin-2 and tenascin-C are largely restricted to developing fetal tissues but become expressed again in granular type I corneal dystrophy and in lattice type I dystrophy. Fibrillin-2, tenascin-C, matrilin-2, and matrilin-4 may be characteristic of the pathogenesis of either the granular

or lattice type I corneal dystrophy, as revealed by immunohistochemical analysis. Each molecule seems to be involved to some degree in the regeneration and reorganization of the corneal matrix in granular and lattice type I dystrophies. However, we observed substantial differences in ECM reconstruction and remodeling between the two dystrophy types. Further experiments are needed to confirm the role of these proteins in the matrix regeneration and repair in corneal stromal dystrophies and to reveal their exact mechanism of action.

ACKNOWLEDGMENTS

The authors would like to thank Anne Seppänen, Anne Mari Haapaniemi and Tünde Terdik for their excellent technical assistance. This work was supported by grants from the Academy of Finland, the Finnish Eye Foundation (to K.K.), and the Korea Research Fund of the University of Debrecen Medical and Health Science Centre (to Sz.F).

REFERENCES

- Weiss JS, Møller HU, Lisch W, Kinoshita S, Aldave AJ, Belin MW, Kivelä T, Busin M, Munier FL, Seitz B, Sutphin J, Bredrup C, Mannis MJ, Rapuano CJ, Van Rij G, Kim EK, Klintworth GK. The IC3D classification of the corneal dystrophies. *Cornea* 2008; 27:S1-83. [PMID: 19337156]
- Stone EM, Mathers WD, Rosenwasser GO, Holland EJ, Folberg R, Krachmer JH, Nichols BE, Gorevic PD, Taylor CM, Streb LM, Fishbaugh JA, Daley TE, Sucheski BM, Sheffield VC. Three autosomal dominant corneal dystrophies map to chromosome 5q. *Nat Genet* 1994; 6:47-51. [PMID: 8136834]
- Munier FL, Korvatska E, Djemaï A, Le Paslier D, Zografos L, Pescia G, Schorderet DF. Keratoepithelin mutations in four 5q31-linked corneal dystrophies. *Nat Genet* 1997; 15:247-51. [PMID: 9054935]
- Klintworth GK. Advances in the molecular genetics of corneal dystrophies. *Am J Ophthalmol* 1999; 128:747-54. [PMID: 10612512]
- Korvatska E, Munier FL, Chaubert P, Wang MX, Mashima Y, Yamada M, Uffer S, Zografos L, Schorderet DF. On the role of kerato-epithelin in the pathogenesis of 5q31-linked corneal dystrophies. *Invest Ophthalmol Vis Sci* 1999; 40:2213-9. [PMID: 10476785]
- Otori T. Electrolyte content of the rabbit corneal stroma. *Exp Eye Res* 1967; 6:356-67. [PMID: 6060547]
- Hassell JR, Birk DE. The molecular basis of corneal transparency. *Exp Eye Res* 2010; 91:326-35. [PMID: 20599432]
- Robertson I, Jensen S, Handford P. TB domain proteins: evolutionary insights into the multifaceted roles of fibrillins and LTBP. *Biochem J* 2011; 433:263-76. [PMID: 21175431]
- Olivieri J, Smaldone S, Ramirez F. Fibrillin assemblies: extracellular determinants of tissue formation and fibrosis. *Fibrogenesis Tissue Repair* 2010; 3:24. [PMID: 21126338]
- Udalova IA, Ruhmann M, Thomson SJ, Midwood KS. Expression and immune function of tenascin-C. *Crit Rev Immunol* 2011; 31:115-45. [PMID: 21542790]
- Chiquet-Ehrismann R, Chiquet M. Tenascins: regulation and putative functions during pathological stress. *J Pathol* 2003; 200:488-99. [PMID: 12845616]
- Chiquet-Ehrismann R, Kalla P, Pearson CA, Beck K, Chiquet M. Tenascin interferes with fibronectin action. *Cell* 1988; 53:383-90. [PMID: 2452695]
- Huang W, Chiquet-Ehrismann R, Moyano JV, Garcia-Pardo A, Orend G. Interference of tenascin-C with syndecan-4 binding to fibronectin blocks cell adhesion and stimulates tumor cell proliferation. *Cancer Res* 2001; 61:8586-94. [PMID: 11731446]
- Ballard VL, Sharma A, Duignan I, Holm JM, Chin A, Choi R, Hajjar KA, Wong SC, Edelberg JM. Vascular tenascin-C regulates cardiac endothelial phenotype and neovascularization. *FASEB J* 2006; 20:717-9. [PMID: 16461331]
- Huang W, Chiquet-Ehrismann R, Moyano JV, Garcia-Pardo A, Orend G. Interference of tenascin-C with syndecan-4 binding to fibronectin blocks cell adhesion and stimulates tumor cell proliferation. *Cancer Res* 2001; 61:8586-94. [PMID: 11731446]
- Brinckmann J, Hunzelmann N, Kahle B, Rohwedel J, Kramer J, Gibson MA, Hubmacher D, Reinhardt DP. Enhanced fibrillin-2 expression is a general feature of wound healing and sclerosis: potential alteration of cell attachment and storage of TGF-beta. *Lab Invest* 2010; 90:739-52. [PMID: 20195245]
- Deák F, Piecha D, Bachrati C, Paulsson M, Kiss I. Primary structure and expression of matrilin-2, the closest relative of cartilage matrix protein within the von Willebrand factor type A-like module superfamily. *J Biol Chem* 1997; 272:9268-74. [PMID: 9083061]
- Piecha D, Muratoglu S, Morgelin M, Hauser N, Studer D, Kiss I, Paulsson M, Deak F. Matrilin-2, a large, oligomeric matrix protein, is expressed by a great variety of cells and forms fibrillar networks. *J Biol Chem* 1999; 274:13353-61. [PMID: 10224097]
- Wagener R, Ehlen HW, Ko YP, Kobbe B, Mann HH, Sengle G, Paulsson M. The matrilin-adaptor proteins in the extracellular matrix. *FEBS Lett* 2005; 579:3323-9. [PMID: 15943978]
- Wagener R, Kobbe B, Paulsson M. Matrilin-4, a new member of the matrilin family of extracellular matrix proteins. *FEBS Lett* 1998; 436:123-7. [PMID: 9771906]
- Klatt AR, Nitsche DP, Kobbe B, Macht M, Paulsson M, Wagener R. Molecular structure, processing, and tissue distribution of matrilin-4. *J Biol Chem* 2001; 276:17267-75. [PMID: 11279097]
- Hegyí Z, Kis G, Holló K, Ledent C, Antal M. Neuronal and glial localization of the cannabinoid-1 receptor in the superficial spinal dorsal horn of the rodent spinal cord. *Eur J Neurosci* 2009; 30:251-62. [PMID: 19614976]
- Klintworth GK. Corneal dystrophies. *Orphanet J Rare Dis* 2009; 4:7. [PMID: 19236704]
- Reinhardt DP, Sasaki T, Dzamba BJ, Keene DR, Chu ML, Göhring W, Timpl R, Sakai LY. Fibrillin-1 and fibulin-2 interact and are colocalized in some tissues. *J Biol Chem* 1996; 271:19489-96. [PMID: 8702639]
- LeBaron RG, Bezverkov KI, Zimmer MP, Pavelec R, Skonier J, Purchio AF. Beta IG-H3, a novel secretory protein inducible by transforming growth factor-beta, is present in normal skin and promotes the adhesion and spreading of dermal

- fibroblasts in vitro. *J Invest Dermatol* 1995; 104:844-9. [[PMID: 7738366](#)]
26. Bae JS, Lee SH, Kim JE, Choi JY, Park RW, Yong Park J, Park HS, Sohn YS, Lee DS, Bae Lee E, Kim IS. Betaig-h3 supports keratinocyte adhesion, migration, and proliferation through alpha3beta1 integrin. *Biochem Biophys Res Commun* 2002; 294:940-8. [[PMID: 12074567](#)]
 27. Ge H, Cao W, Leng F, Chen W, Liu P, Chen W. Modified BIGH3 with an RGDGRGD motif promotes human corneal epithelial cell adhesion and migration in vitro. *Curr Eye Res* 2008; 33:215-23. [[PMID: 18350432](#)]
 28. Schmitt-Bernard CF, Chavanieu A, Herrada G, Subra G, Arnaud B, Demaille JG, Calas B, Argilés A. BIGH3 (TGFB1) Arg124 mutations influence the amyloid conversion of related peptides in vitro. *Eur J Biochem* 2002; 269:5149-56. [[PMID: 12392546](#)]
 29. Resch MD, Schlötzer-Schrehardt U, Hofmann-Rummelt C, Kruse FE, Seitz B. Alterations of epithelial adhesion molecules and basement membrane components in lattice corneal dystrophy (LCD). *Graefes Arch Clin Exp Ophthalmol* 2009; 247:1081-8. [[PMID: 19190930](#)]
 30. Dahlbäck K, Sakai L. Immunohistochemical studies on fibrillin in amyloidosis, lichen ruber planus and porphyria. *Acta Derm Venereol* 1990; 70:275-80. [[PMID: 1699374](#)]
 31. Schlötzer-Schrehardt U, Dietrich T, Saito K, Sorokin L, Sasaki T, Paulsson M, Kruse FE. Characterization of extracellular matrix components in the limbal epithelial stem cell compartment. *Exp Eye Res* 2007; 85:845-60. [[PMID: 17927980](#)]
 32. Fagerholm P. Phototherapeutic keratectomy: 12 years of experience. *Acta Ophthalmol Scand* 2003; 81:19-32. [[PMID: 12631015](#)]
 33. Maseruka H, Bonshek RE, Tullo AB. Tenascin-C expression in normal, inflamed, and scarred human corneas. *Br J Ophthalmol* 1997; 81:677-82. [[PMID: 9349157](#)]
 34. Meltendorf C, Burbach GJ, Bühren J, Bug R, Ohrloff C, Deller T. Corneal femtosecond laser keratotomy results in isolated stromal injury and favorable wound-healing response. *Invest Ophthalmol Vis Sci* 2007; 48:2068-75. [[PMID: 17460262](#)]
 35. Sumioka T, Fujita N, Kitano A, Okada Y, Saika S. Impaired angiogenic response in the cornea of mice lacking tenascin C. *Invest Ophthalmol Vis Sci* 2011; 52:2462-7. [[PMID: 21087965](#)]
 36. Ljubimov AV, Burgeson RE, Butkowski RJ, Couchman JR, Wu RR, Ninomiya Y, Sado Y, Maguen E, Nesburn AB, Kenney MC. Extracellular matrix alterations in human corneas with bullous keratopathy. *Invest Ophthalmol Vis Sci* 1996; 37:997-1007. [[PMID: 8631643](#)]
 37. Akhtar S, Bron AJ, Hawksworth NR, Bonshek RE, Meek KM. Ultrastructural morphology and expression of proteoglycans, betaig-h3, tenascin-C, fibrillin-1, and fibronectin in bullous keratopathy. *Br J Ophthalmol* 2001; 85:720-31. [[PMID: 11371495](#)]
 38. Maseruka H, Ridgway A, Tullo A, Bonshek R. Developmental changes in patterns of expression of tenascin-C variants in the human cornea. *Invest Ophthalmol Vis Sci* 2000; 41:4101-7. [[PMID: 11095602](#)]
 39. Kabosova A, Azar DT, Bannikov GA, Campbell KP, Durbeej M, Ghohestani RF, Jones JC, Kenney MC, Koch M, Ninomiya Y, Patton BL, Paulsson M, Sado Y, Sage EH, Sasaki T, Sorokin LM, Steiner-Champliand MF, Sun TT, Sundarraj N, Timpl R, Virtanen I, Ljubimov AV. Compositional differences between infant and adult human corneal basement membranes. *Invest Ophthalmol Vis Sci* 2007; 48:4989-99. [[PMID: 17962449](#)]
 40. Tuori A, Virtanen I, Aine E, Uusitalo H. The expression of tenascin and fibronectin in keratoconus, scarred and normal human cornea. *Graefes Arch Clin Exp Ophthalmol* 1997; 235:222-9. [[PMID: 9143890](#)]
 41. Tiitta O, Wahlström T, Paavonen J, Linnala A, Sharma S, Gould VE, Virtanen I. Enhanced tenascin expression in cervical and vulvar koilocytotic lesions. *Am J Pathol* 1992; 141:907-13. [[PMID: 1384340](#)]
 42. Piecha D, Wiberg C, Mörgelin M, Reinhardt DP, Deák F, Maurer P, Paulsson M. Matrilin-2 interacts with itself and with other extracellular matrix proteins. *Biochem J* 2002; 367:715-21. [[PMID: 12180907](#)]
 43. Malin D, Sonnenberg-Riethmacher E, Guseva D, Wagener R, Aszódi A, Irintchev A, Riethmacher D. The extracellular-matrix protein matrilin 2 participates in peripheral nerve regeneration. *J Cell Sci* 2009; 122:995-1004. [[PMID: 19295126](#)]
 44. Ichikawa T, Suenaga Y, Koda T, Ozaki T, Nakagawara A. DeltaNp63/BMP-7-dependent expression of matrilin-2 is involved in keratinocyte migration in response to wounding. *Biochem Biophys Res Commun* 2008; 369:994-1000. [[PMID: 18328806](#)]
 45. Sharma MK, Watson MA, Lyman M, Perry A, Aldape KD, Deák F, Gutmann DH. Matrilin-2 expression distinguishes clinically relevant subsets of pilocytic astrocytoma. *Neurology* 2006; 66:127-30. [[PMID: 16401863](#)]
 46. Szabó E, Korpos E, Batmunkh E, Lotz G, Holczbauer A, Kovalszky I, Deák F, Kiss I, Schaff Z, Kiss A. Expression of matrilin-2 in liver cirrhosis and hepatocellular carcinoma. *Pathol Oncol Res* 2008; 14:15-22. [[PMID: 18386166](#)]

Articles are provided courtesy of Emory University and the Zhongshan Ophthalmic Center, Sun Yat-sen University, P.R. China. The print version of this article was created on 14 July 2012. This reflects all typographical corrections and errata to the article through that date. Details of any changes may be found in the online version of the article.